Ruthenium arene complexes in the treatment of 3D models of Head and Neck Squamous Cell Carcinomas

Melissa Santi,[1,2] Ana Katrina Mapanao,[1,3] Lorenzo Biancalana,[4] Fabio Marchetti[4*] and Valerio Voliani[1*]

[1]Center for Nanotechnology Innovation@NEST, Istituto Italiano di Tecnologia, Piazza San Silvestro, 12-56126, Pisa, Italy.

[2] Istituto Nanoscienze-CNR and Scuola Normale Superiore, Piazza San Silvestro 12, 56127, Pisa, Italy.

[3]NEST-Scuola Normale Superiore, Piazza San Silvestro, 12-56126, Pisa, Italy.

[4] Department of Chemistry and Industrial Chemistry, University of Pisa, Via Moruzzi 13, 56124 Pisa, Italy.

Corresponding authors: fabio.marchetti1974@unipi.it, valerio.voliani@iit.it

ABSTRACT

Current chemotherapy for head and neck squamous cell carcinomas (HNSCCs) are based on cisplatin, which is usually associated to severe side effects. In general, the exploration for metal-based alternatives to cisplatin has resulted in the development of a series of ruthenium complexes that are able to produce a safe therapeutic action against some neoplasms, among which are lung and ovarian cancers. Here, we evaluate the efficacy of well defined, easily available and robust ruthenium(II) η^6-arene compounds on 3D models of HNSCCs with or without human papillomavirus (HPV) infection and compare their effects to the state-of-the-art RAPTA-C, a promising ruthenium compound with known anti-cancer activity. One of the compounds induces a significant therapeutic action especially on HPV negative carcinoma. Besides viability and repopulation evaluations, we performed quantitative analysis of the internalized Ru compounds to further validate our findings and elucidate the possible mechanisms of action. These results show that Ru arene compounds represent a promising alternative for the treatment of HNSCCs and pave the way for the composition of innovative (co)therapies.

Keywords: HNSCCs; Ruthenium arene complexes; Cisplatin; chemotherapy; 3D models

INTRODUCTION

Head and neck squamous cell carcinomas (HNSCCs) are a wide class of malignancies that involve the oro-pharyngeal apparatus including tongue, pharynx, larynx, and salivary glands.[1] It accounts for thousands of new cases every year and is one of the most common cancer types.[2] It is mainly caused by unhealthy lifestyle such as excessive use of alcohol and tobacco, even if a correlation occurs between the onset of head and neck cancers and the presence of human Papillomavirus (HPV) infections.[3] The presence of HPV usually implies a different outcome to treatments. HPV-positive subjects are generally more sensitive to therapies and show a

better prognosis.[4] In contrast, HPV-negative tumors are typically more aggressive and usually have a poor prognosis with high risk of recurrence/metastasis (R/M HNSCCs).[5] The main treatment for both ±HPV HNSCCs is still based on primary surgery combined with chemo- and/or radio-therapy.[6] On this regard, platinum-based drugs are widely employed for the treatment of many types of tumors including head and neck, due to their wide spectrum of activity.[7] However, despite the consolidated use of the cisplatin family for chemotherapy, platinum drugs demonstrated a significant systemic toxicity, including nephrotoxicity and neurotoxicity.[8] On this hand, considerable efforts have been recently made to identify other approaches to produce safer forms or new metal-based alternatives to cisplatin.[9–11] In the last years, ruthenium(II) arene complexes have demonstrated to be a valid alternative to cisplatin and related compounds for the treatment of some solid neoplasms, among which are lung and ovarian carcinomas.[12,13] Moreover, the versatility of the Ru-arene scaffold enables the production of several molecules comprising tunable actions for the treatment and diagnosis of tumors.[12–14] In fact, [RuCl$_2$(PTA)(η^6-p-cymene)], a Ru(II) complex comprising the amphiphilic phosphine 1,3,5-triaza-7-phosphatricyclo[3.3.1.1]decane (PTA), also known as RAPTA-C (Figure 1), has emerged as one of the most promising ruthenium-arene anticancer candidates, and currently points to clinical trials.[15] Although the mechanism of action is not yet totally clear, RAPTA-C should primarily inhibit angiogenesis rather than induce cell apoptosis/necrosis.[16] Indeed, while it is predominantly non-toxic for most of cancer cell lines, it showed good *in vivo* anticancer activity.[17] On the other hand, the simple and versatile structure of RAPTA-C have encouraged the development of related, optimized RAPTA-C analogs.[18,19] RAPTA-C conjugated with polylactic acid (PLA) micelles have been recently tested for antimetastatic activity in 3D ovarian and breast cancer cell models.[16,20,21] Recently, some of us reported a new series of cationic ruthenium(II) p-cymene complexes bearing α-diimine ligands, of general formula [RuCl{$\kappa^2 N$-(HC=NR)$_2$}(η^6-p-cymene)]NO$_3$, has been reported by some of us (Figure 1).[22,23] These organometallic species can be prepared from commercial precursors through a straightforward procedure, and possess a good solubility in water (> 5 mM) and a high stability in aqueous media under physiological conditions. These are important pre-requisites for a potential metal drug, and, among the multitude of ruthenium arene compounds investigated for their biological action, only a limited number fully meets such criteria.[24–26] The ruthenium α-diimine compounds manifested an *in vitro* cytotoxicity on ovarian cancer cell lines which is strongly dependent on the nitrogen substituent R. For instance, **RuCy** (R = cyclohexyl) is highly cytotoxic both on cisplatin sensitive A2780 and cisplatin-resistant A2780cisR ovarian cancer cells (IC$_{50}$ ≈ 3-4 μM after 72 h incubation) while the pH sensitive **RuPh** (R = 4-hydroxyphenyl) is not (IC$_{50}$ > 200 μM). Here, **RuCy** and **RuPh** have been evaluated for the treatment of two different HNSCC cell lines: SCC-25, which is HPV-negative, and UPCI:SCC-154, which is HPV-positive. We assessed the efficacy of the two compounds by employing both 2D and standardized 3D cancer models of the two cell lines, and compared the findings with those obtained

with the state-of-the-art **RAPTA-C**.[27] 3D cell models better represent the complexity of tumor environment with respect to 2D cell culture and provide more reliable information about the performances of tested drugs within the 3R's concept.[28] It should be noted that apart from the previously mentioned RAPTA-C derivatized micelles,[20,21,29] only few Ru(II) arene compounds have been tested on 3D cellular models to date.[30–32] Furthermore, we compared the action of ruthenium compounds on an endothelial cell line (bEnd.3) and quantitatively assessed their internalization in all the cell lines to further validate our findings and elucidate possible mechanisms of action. Our results confirm the potentiality of molecular ruthenium compounds for the development of safer chemo-treatment for HNSCCs, providing the basis for the composition of innovative (co)chemotherapies based on nano-technology.[10,33–35]

RESULTS AND DISCUSSION

Cytotoxic effect of ruthenium compounds on 2D cell cultures

As a first approach, the efficacy of ruthenium complexes on HNSCCs has been evaluated on 2D cell cultures. Cells have been treated with increasing concentrations of **RuCy**, **RuPh** and **RAPTA-C,** ranging from 1 µM to 400 µM. Briefly, cells were incubated with the Ru-complexes for 2 h, washed and the viability was monitored after 24, 48 and 72h (**Figure 2** and **Figure S2**).
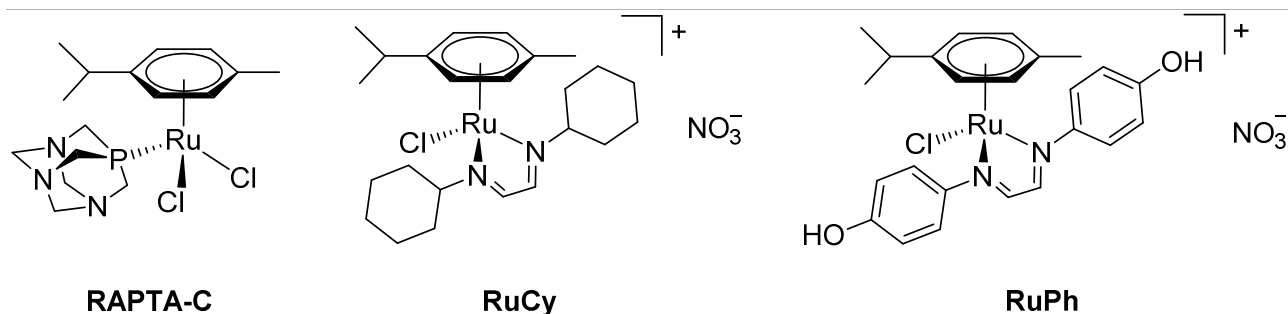
Figure 1: Structure of RAPTA-C and Ru(II) arene α-diimine complexes used in this study.

Noticeably, our incubation procedure involved a short drug exposure timeframe to better identify and evaluate the initial biological effects of the complexes and to avoid complications (misinterpretations?) caused by prolonged and continuous chemical exposure. IC$_{50}$ values after 72h are reported in **Table 1**. **RuCy** exhibited a cytotoxic effect against all cell lines, including on bEnd.3 endothelial cells, albeit low. **RuPh** and **RAPTA-C** did not show any cytotoxic effect at least up to the concentration of 400 µM. **RuPh** and **RAPTA-C** did not affect the viability of the cancer cell lines nor of the bEnd.3 used as endothelial control. The behavior of the three Ru(II) complexes is aligned to that observed on other cell types, following 72 h incubation.[15] This finding agrees

with the supposed mechanism of action of **RAPTA-C**, eliciting main action on the extracellular matrix at the endothelial level, and confirms that 3D cancer models are pivotal for the evaluation of these compounds.
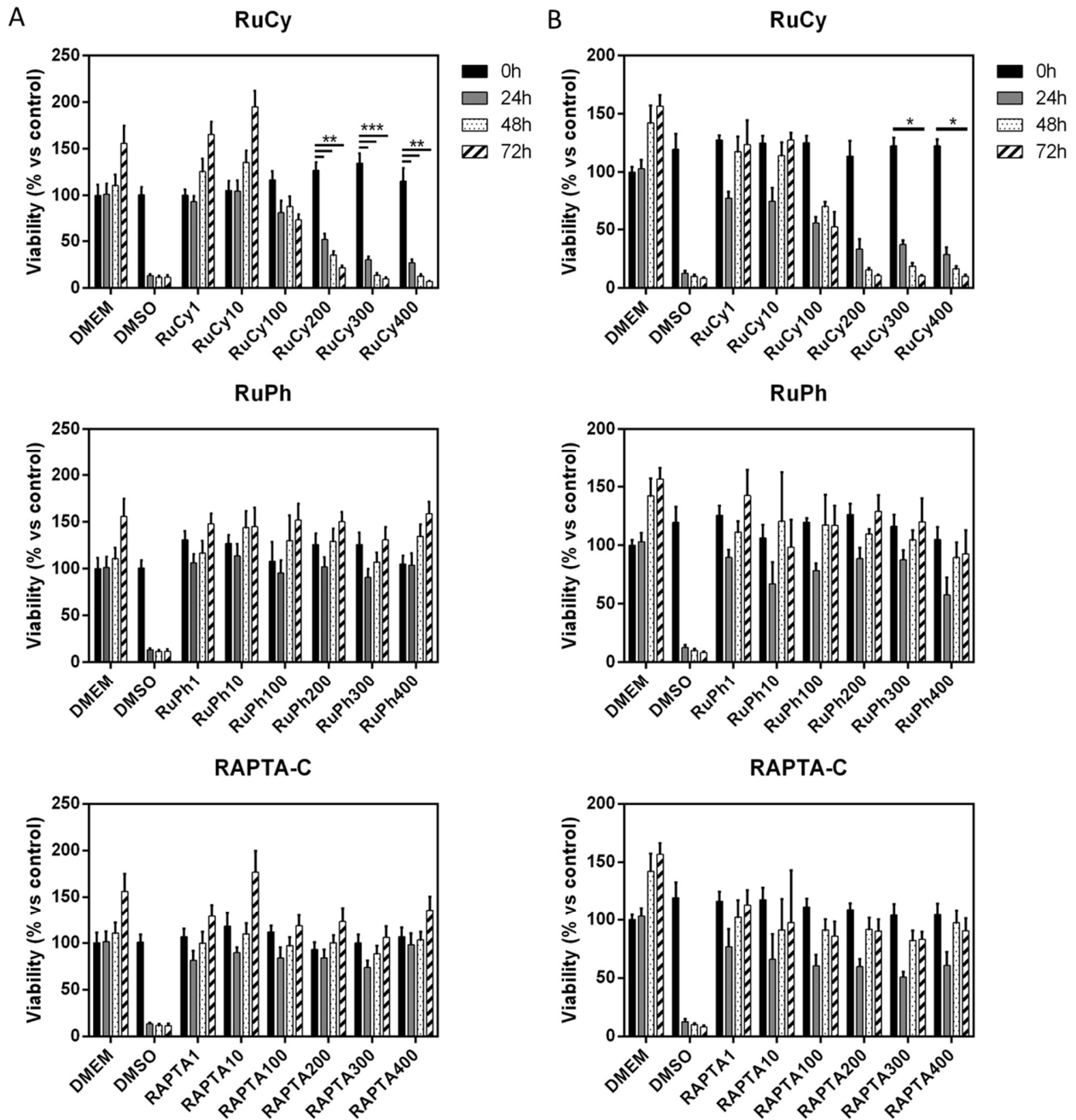

Figure 2: Cytotoxicity of ruthenium compounds on HNSCCs cell lines. (A) SCC-25 and (B) UPCI:SCC-154 cells were treated with increasing concentrations (in µM) of **RuCy**, **RuPh** or **RAPTA-C** for 2h at 37 °C. Then, cells were

washed and medium was replaced with fresh one. Viability was measured by WST-8 assay during time until 72 h and data were normalized to the viability of control cells (treated only with medium - DMEM). Cells treated with 20% of DMSO were used as positive control of the experiment. Results are the average of three independent experiments and error bars state the standard deviation. One-way ANOVA with Dunnett's test vs. 0 h. *$p < 0.05$, **$p < 0.02$, ***$p < 0.0001$.

Table 1. IC$_{50}$ values for ruthenium compounds determined after 2 h exposure to the drug then 72 h with fresh medium.

	IC$_{50}$ after 72 h (µM)		
	SCC-25	*UPCI:SCC-154*	*bEnd.3*
RuCy	78.5	91.8	186.5
RuPh	>400	>400	>400
RAPTA-C	>400	>400	>400

Then, the effect of the compounds was evaluated on the cell migration ability after the treatment. This investigation is of special interest since **RAPTA-C** can be poorly internalized in cells.[17] Thus, a migration assay on SCC-25 cells has been performed. Note that the scratch assay was not performed on UPCI:SCC-154 due to their growth modality, in which the cells form islands of several layers instead of a compact and dispersed monolayer (**Figure S2**). Briefly, seeded cells have been scratched from the plates with a tip and their ability to repopulate the region has been observed after the treatment with ruthenium complexes (**Figure 3**). **RAPTA-C** and **RuPh** did not influence SCC-25 cells, which were able to invade again the selected region after 24 h. Interestingly, we observed a severe influence of **RuCy**, confirming its cytotoxic effect, probably due to a different mechanism of action with respect to the other two compounds. The same experiment performed on bEnd.3 cells as a control resulted in similar outcomes (**Figure S3**).
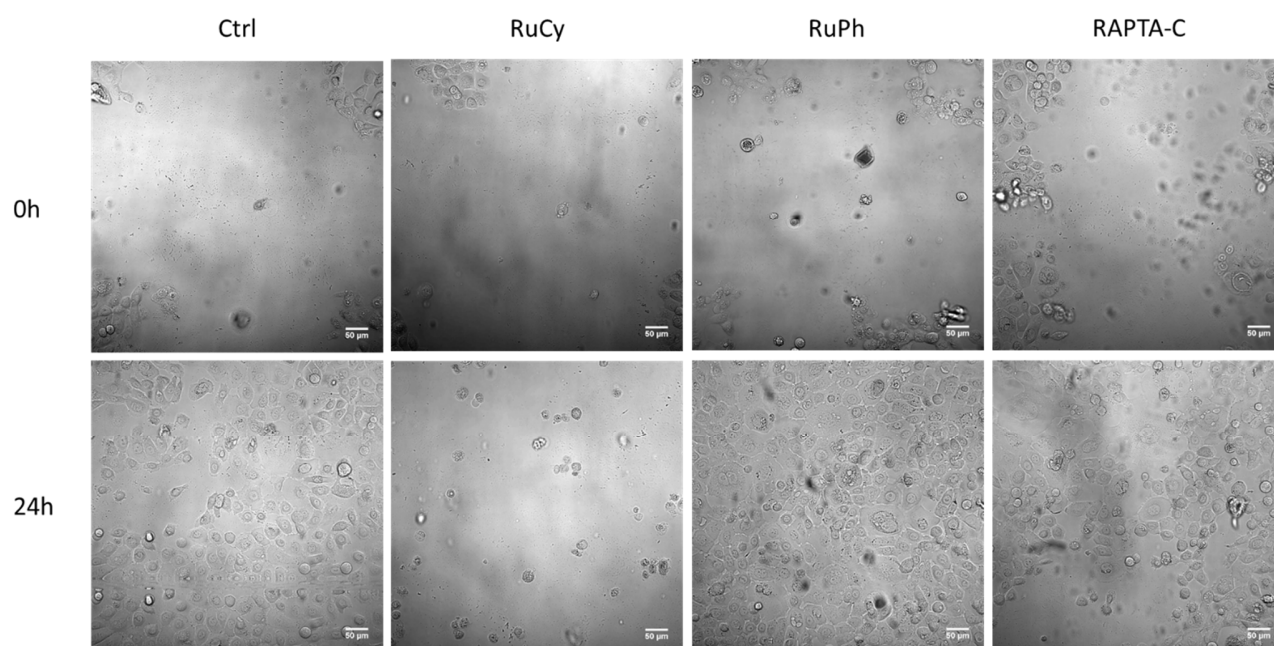
Figure 3: Migration assay. Bright field images of SCC-25 cells taken with a confocal microscope before and after the treatment with ruthenium compounds. Cells were seeded in Willco dishes and scratched from the glass with a tip. Then cells were treated with 200 μM of each ruthenium compound for 2h, and then observed under the microscope after 24h. Scale bar: 50 μm.

Internalization in 2D cell cultures

Taken together, the results obtained from viability and migration experiments suggest a different mechanism of action for **RuCy**. Since we performed all the experiments by treating the cells with only 2h incubation, at variance to the typical 72h protocol, it is reasonable to assume that the outcomes are associated to the internalized compounds rather than their prolonged interaction with cells in the culture medium. Therefore, the different cytotoxic performance of RuCy, RuPh and RAPTA-C can be attributed to a different ability of the Ru(II) complexes to be internalized in cells. In order to shed light on this point, the internalization rate of the complexes has been quantitatively measured in both HNSCCs cell lines and compared to the control compound, **RAPTA-C**. In addition, the endothelial bEnd.3 cell line has been employed for comparison. Each cell lines (with a comparable number of seeded cells) was treated with two concentrations of ruthenium complexes, 50 μM and 100 μM for 2 h, and the internalization was measured by ICP-MS (**Table 2**). Interestingly, all compounds were internalized in both HNSCCs cell lines in a concentration-dependent fashion, with a general higher internalization for UPCI:SCC-154.

Despite being a rather hydrophilic compound (log P_{ow} = − 0.8),[23] **RuCy** showed a higher internalization than both **RuPh** and **RAPTA-C** in the two cancer cell lines at both levels of concentration, and in the bEnd.3 cell line at 100 µM. These results indicate that **RuCy** is extensively internalized in cancer cells where it exerts its cytotoxic activity. Overall, **RuCy** exibited a more pronounced cytotoxic effect on SCC-25 despite the minor internalization with respect to UPCI:SCC-154. On the other hand, **RuPh** was also internalized in cells but to a lesser extent (about 40% and 50% less for SCC25 and UPCI:SCC-154, respectively) and showed no biological action. Finally, we observe that **RAPTA-C** is generally not able to be internalized in cells, except for a small uptake in UPCI:SCC-154 cell line.

Table 2: Quantification of ruthenium in cells by ICP-MS analysis.

	bEnd.3	*SCC-25*	*UPCI:SCC-154*
	mass Ru (ng)	mass Ru (ng)	mass Ru (ng)
RuCy 50	10.0 ± 0.8	26.5 ± 2.8	38.9 ± 9.6
RuCy 100	22.3 ± 2.1	54.2 ± 1.8	76.9 ± 6.3
RuPh 50	24.7 ± 2.8	7.8 ± 0.4	21.5 ± 5.9
RuPh 100	28.6 ± 3.1	12.5 ± 0.5	40.4 ± 18.5
RAPTA-C 50	0.32 ± 0.11	0.4 ± 0.02	2.9 ± 0.2
RAPTA-C 100	0.54 ± 0.04	1.6 ± 0.5	8.0 ± 1.7

Cytotoxic effect of ruthenium compounds on 3D cell cultures

Despite a variety of ruthenium arene complexes has been proposed as potential anticancer drugs, there is a paucity of information in the literature concerning the behavior of this family of metal compounds in 3D models. Therefore, we assessed the Ru-complexes presented herein on 3D cell models. The spheroids represent a significant tumor model as the three-dimensional structures better cover the nano-bio interactions and cancer behaviors compared to 2D cultures. Remarkably, the extracellular matrix environment is well represented in spheroids, which is of particular importance for the assessment of Ru-complexes.[36] HNSCCs spheroids have been produced and characterized following an established protocol.[27] In agreement with the previous findings, they were treated with ruthenium compounds at a single concentration of 200 µM and we followed the viability during time (**Figure 4 A**, **B** and **C**). Also on 3D structures, **RuPh** did not show any

significant toxic action also on 3D structures. On the other hand, **RuCy** confirmed to be toxic for all cell lines with a more pronounced effect for SCC-25, thereby confirming the findings collected on 2D cells. Differently from what evidenced in 2D cell cultures, the effect of **RuCy** on SCC-25 spheroids occurred starting from 48h. UPCI:SCC-154 instead, are sensible starting from 24 h. These results could be explained by the higher RuCy internalization in UPCI:SCC-154 cells respect to SCC-25 that lead to a marked and faster activity on 3D models. These differences were not discriminated in 2D cultures, highlighting the pivotal importance of three-dimensional models in pre-clinical cancer research. Interestingly we also observed an effect of **RAPTA-C** on 3D models of UPCI:SCC-154. This cell line is characterized by the presence of an abundant extracellular matrix, which is especially evident in the spheroids (**Figure 4D**). Thus, the action of **RAPTA-C** can be associated to the extracellular environment, as already reported *in vivo* or *in ovo* for other tumor types.[37] Remarkably, analogous complexes [RuCl(N,N)(η^6-p-cymene)]$^+$ (N,N = dipyrido[3,2-a:2',3'-c]phenazine type ligands) showed a considerably lower effect on viability of 3D spheroids of PANC-1 pancreatic and melanoma A375 cells if compared to their behavior on related 2D models.[30,32]
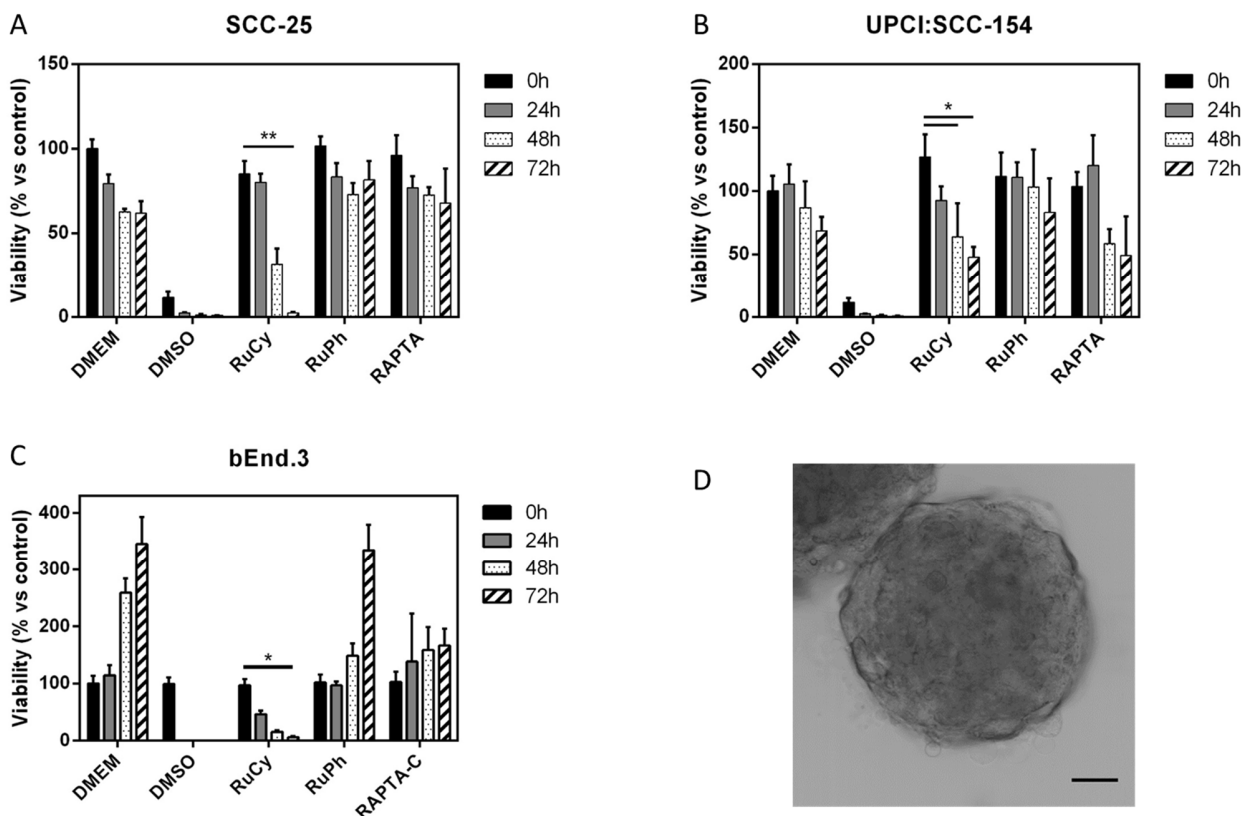
Figure 4: Viability assay on 3D spheroids of HNSCCs cell lines. Spheroids of (A) SCC-25, (B) UPCI:SCC-154 or (C) bEnd.3 were treated for 2 h with different ruthenium compounds at 200 μM. Then spheroids were washed and

maintained in fresh medium. After 24, 48 and 72 h, viability was measured with CellTiter-Glo® 3D Cell Viability kit. Two-way ANOVA (Dunnett's multiple comparison test) vs. 0h. *$p < 0.05$, **$p < 0.02$. (D) Bright-field image of a spheroid of UPCI:SCC-154. Scale bar: 50 µm.

CONCLUSION

In summary, we tested a selection of easily available and water stable ruthenium arene complexes on 3D models of HPV-positive and HPV-negative HNSCCs and compared our findings with **RAPTA-C** as gold standard for this family of compounds. Remarkably, this is the first time that ruthenium compounds have been tested on HNSCCs models and, more in general, investigations of ruthenium arene compounds on 3D cell models are exceedingly rare. Among the tested compounds, **RuCy** displayed a promising cytotoxic effect on all tested cell lines both in 2D and 3D cell cultures, and, thus, represents a potential alternative to current cisplatin-based therapies. It is worth to notice that **RAPTA-C** is not cytotoxic on 2D cells while evidenced an encouraging effect on spheroids of UPCI:SCC-154, suggesting that sophisticated biological models are crucial for the assessment of the anticancer action of ruthenium arene. Overall, our findings constitute a starting point for the development of a new approach for the efficient (co)treatment of HNSCCs.

Conflict of Interest

The authors declare no conflict of interest.

Notes

The raw and processed data required to reproduce these findings are available on request to the Authors.

MATERIALS AND METHODS

Synthesis of ruthenium arene complexes

Ruthenium arene complexes **RuCy**, **RuPh** and **RAPTA-C**, were synthesized following the respective literature procedures.[21,23]

Cell culture

Human squamous cell carcinoma SCC-25 and UPCI-SCC-154 and endothelial cell bEnd.3 were purchased from the American Type Culture Collection (ATCC). SCC-25 were maintained in a complete growth medium composed of a 1:1 mixture of Dulbecco's modified Eagle's medium and Ham's F12 medium while UPCI-SCC-154 and bEnd.3 were growth in Dulbecco's modified Eagle medium (DMEM) from Invitrogen (Carlsbad, CA). Both growth media were supplemented with 10% fetal bovine serum (FBS), 4mM L-glutamine, 1 mM sodium pyruvate, 100 U/mL penicillin, and 100 mg/mL streptomycin (Invitrogen). SCC-25 medium was also supplemented with 400 ng/mL of hydrocortisone. Cells were maintained at 37 °C in a humidified 5% CO_2 atmosphere.

Production of 3D spheroids

HNSCCs and bEnd.3 spheroids were produced following a standardized protocol.[27] Briefly, cells were collected from plate and resuspended in fresh medium, counted and the suspension was adjusted to a final concentration of 1×10^6 cells/mL. Then, 10 μL (for SCC-25 and bEnd.3) or 20 μL (for UPCI-SCC-154) of cells were placed on the lid of a 100-mm cell culture dish that was flipped into the chamber containing 10 mL of PBS. Cells were left to settle into the drops until they formed a sheet and then were transferred to a 100 mm suspension culture dish with cell culture medium after 3 days. Finally, cell aggregates were placed inside a CO_2 incubator with an orbital shaker (70 rpm) for 24 h to induce the formation of the proper spherical shape.

Viability assay on 2D and 3D cell cultures

Viability experiments on 2D cell cultures were performed using a tetrazolium salt, 2-(2-methoxy-4-nitrophenyl)-3-(4-nitrophenyl)-5-(2,4-disulfophenyl)-2H tetrazolium, and monosodium salt (WST-8) assay. All types of cells were seeded in 96-well plates for 24 h to reach 80-90% of confluency. Then each cell line was treated with increasing concentrations of ruthenium compounds for 2 h at 37°C. after this time, cells were washed twice with phosphate-buffered saline (PBS) and fresh medium with 2% FBS was added. Viability was monitored after 24, 48 and 72 h and referred to the viability of control cells without treatments set as 100% (DMEM). We also added a positive control represented by cells treated with 20% of DMSO. For each experimental time point cells were incubated with WST-8 reagent (100 μL) and 2% serum-containing medium (90 μL) for 2 h. Absorbance (450 nm) was measured using a microplate reader (Glomax Discovery, Promega, Madison, WI, USA). Data represent the average of three independent experiments. Error bars represent the standard deviation from three independent experiments. The viability of 3D spheroids was followed by quantifying the adenosine triphosphate (ATP) content of metabolically active cells using CellTiter-Glo® 3D (Promega), which was used as per manufacturer's instructions.

Migration assay

SCC-25 and bEnd.3 cells were seeded 24 h before the experiments into a glass-bottom Petri dish (WillCo-dish GWSt-3522) to reach 80–90% of confluence. Samples were scratched with a tip to form a cross at the center of the plates. Bright-field images of the scratched regions were taken with a confocal microscope (Zeiss Axio Vert.A1). Cells were treated with ruthenium compounds at 200 µM for 2h at 37°C, washed twice with PBS and finally added with fresh culture medium. Images were again taken after 24 h to see the ability of the cells to migrate or repopulate the scratched region. Samples treated with ruthenium compounds were compared to untreated cells.

ICP-MS analysis

All cell lines were seeded 24 h before incubation with the complexes in 24-well plates to reach 80-90 % of confluency. Cells were treated with ruthenium compounds at two different concentrations, 50 µM and 100 µM, for 2 h at 37°C. Afterwards, cells were washed twice with PBS and 200 µL of aqua regia were added to each well. The solution was placed in a glass tube and samples were digested at 200 °C for 15 minutes. The resulting solutions were diluted to 2 mL with ICP-MS grade water. The detected amount of ruthenium was evaluated with respect to a standard calibration curve and results are reported with the standard deviation obtained from three independent samples.

REFERENCES

[1]   Chow LQM. Head and neck cancer. N Engl J Med 2020;382:60–72. doi:10.1056/NEJMra1715715.

[2]   Siegel RL, Miller KD, Jemal A. Cancer statistics, 2019. CA Cancer J Clin 2019;69:7–34. doi:10.3322/caac.21551.

[3]   R.G. M, R.S. B, A.F. O. Human papillomavirus and head and neck cancer: Epidemiology and molecular biology. Head Neck 1998;20:250–65. doi:10.1002/(SICI)1097-0347(199805)20:3<250::AID-HED11>3.0.CO;2-O.

[4]   Rieckmann T, Tribius S, Grob TJ, Meyer F, Busch CJ, Petersen C, et al. HNSCC cell lines positive for HPV and p16 possess higher cellular radiosensitivity due to an impaired DSB repair capacity. Radiother Oncol 2013;107:242–6. doi:10.1016/j.radonc.2013.03.013.

[5]   Lala M, Chirovsky D, Cheng JD, Mayawala K. Clinical outcomes with therapies for previously treated recurrent/metastatic head-and-neck squamous cell carcinoma (R/M HNSCC): A systematic literature review. Oral Oncol 2018;84:108–20. doi:10.1016/j.oraloncology.2018.07.005.

[6]   Busch C-J, Becker B, Kriegs M, Gatzemeier F, Krüger K, Möckelmann N, et al. Similar cisplatin sensitivity of HPV-positive and -negative HNSCC cell lines. Oncotarget 2016;7:35832–42. doi:10.18632/oncotarget.9028.

[7]   Duan X, He C, Kron SJ, Lin W. Nanoparticle formulations of cisplatin for cancer therapy. Wiley Interdiscip Rev Nanomedicine Nanobiotechnology 2016;8:776–91. doi:10.1002/wnan.1390.

[8]   Sacco AG, Cohen EE. Current Treatment Options for Recurrent or Metastatic Head and Neck Squamous Cell Carcinoma. J Clin Oncol 2015;33:3305–13. doi:10.1200/JCO.2015.62.0963.

[9]   Santi M, Mapanao AK, Cassano D, Vlamidis Y, Cappello V, Voliani V. Endogenously-Activated Ultrasmall-in-Nano Therapeutics: Assessment on 3D Head and Neck Squamous Cell Carcinomas. Cancers (Basel) 2020;12:1063. doi:10.3390/cancers12051063.

[10]   Mapanao AK, Santi M, Voliani V. Combined chemo-photothermal treatment of three-dimensional head and neck squamous cell carcinomas by gold nano-architectures. J Colloid Interface Sci 2021;582:1003–11. doi:10.1016/j.jcis.2020.08.059.

[11]   Ndagi U, Mhlongo N, Soliman ME. Metal complexes in cancer therapy – An update from drug design perspective. Drug Des Devel Ther 2017;11:599–616. doi:10.2147/DDDT.S119488.

[12]   Meier-Menches SM, Gerner C, Berger W, Hartinger CG, Keppler BK. Structure-activity relationships for ruthenium and osmium anticancer agents-towards clinical development. Chem Soc Rev 2018;47:909–28. doi:10.1039/c7cs00332c.

[13]   Thota S, Rodrigues DA, Crans DC, Barreiro EJ. Ru(II) Compounds: Next-Generation Anticancer Metallotherapeutics? J Med Chem 2018;61:5805–21. doi:10.1021/acs.jmedchem.7b01689.

[14]   Kenny RG, Marmion CJ. Toward Multi-Targeted Platinum and Ruthenium Drugs - A New Paradigm in Cancer Drug Treatment Regimens? Chem Rev 2019;119:1058–137. doi:10.1021/acs.chemrev.8b00271.

[15]   Murray BS, Babak M V., Hartinger CG, Dyson PJ. The development of RAPTA compounds for the treatment of tumors. Coord Chem Rev 2016;306:86–114. doi:10.1016/j.ccr.2015.06.014.

[16]   Nowak-Sliwinska P, Van Beijnum JR, Casini A, Nazarov AA, Wagnières G, Van Den Bergh H, et al. Organometallic ruthenium(II) arene compounds with antiangiogenic activity. J Med Chem 2011;54:3895–902. doi:10.1021/jm2002074.

[17]   Weiss A, Berndsen RH, Dubois M, Müller C, Schibli R, Griffioen AW, et al. In vivo anti-tumor activity of the organometallic ruthenium(ii)-arene complex [Ru(η6-p-cymene)Cl2(pta)] (RAPTA-C) in human ovarian and colorectal carcinomas. Chem Sci 2014;5:4742–8. doi:10.1039/c4sc01255k.

[18]   Płotek M, Starosta R, Komarnicka UK, Skórska-Stania A, Kołoczek P, Kyzioł A. Ruthenium(II) piano stool coordination compounds with aminomethylphosphanes: Synthesis, characterisation and preliminary biological study in vitro. J Inorg Biochem 2017;170:178–87. doi:10.1016/j.jinorgbio.2017.02.017.

[19]   Aliende C, Pérez-Manrique M, Jalón FA, Manzano BR, Rodríguez AM, Cuevas JV, et al. Preparation of new half sandwich ruthenium arene complexes with aminophosphines as potential chemotherapeutics. J Inorg Biochem 2012;117:171–88. doi:10.1016/j.jinorgbio.2012.07.022.

[20]   Lu M, Chen F, Noy J-M, Lu H, Stenzel MH. Enhanced Antimetastatic Activity of the Ruthenium Anticancer Drug RAPTA-C Delivered in Fructose-Coated Micelles. Macromol Biosci 2017;17:1600513. doi:10.1002/mabi.201600513.

[21]   Lu M, Henry CE, Lai H, Khine YY, Ford CE, Stenzel MH. A new 3D organotypic model of ovarian cancer to help evaluate the antimetastatic activity of RAPTA-C conjugated micelles. Biomater Sci 2019;7:1652–60. doi:10.1039/c8bm01326h.

[22]   Biancalana L, Batchelor LK, Ciancaleoni G, Zacchini S, Pampaloni G, Dyson PJ, et al. Versatile coordination of acetazolamide to ruthenium(II) p-cymene complexes and preliminary cytotoxicity studies. Dalt Trans 2018;47:9367–84. doi:10.1039/c8dt01555d.

[23] Biancalana L, Batchelor LK, Funaioli T, Zacchini S, Bortoluzzi M, Pampaloni G, et al. α-Diimines as Versatile, Derivatizable Ligands in Ruthenium(II) p-Cymene Anticancer Complexes. Inorg Chem 2018;57:6669–85. doi:10.1021/acs.inorgchem.8b00882.

[24] Keller S, Ong YC, Lin Y, Cariou K, Gasser G. A tutorial for the assessment of the stability of organometallic complexes in biological media. J Organomet Chem 2020;906:121059. doi:10.1016/j.jorganchem.2019.121059.

[25] Notaro A, Gasser G, Castonguay A. Note of Caution for the Aqueous Behaviour of Metal-Based Drug Candidates. ChemMedChem 2020;15:345–8. doi:10.1002/cmdc.201900677.

[26] Biancalana L, Pampaloni G, Zacchini S, Marchetti F. One pot conversion of acetyl chloride to dehydroacetic acid and its coordination in a ruthenium(II) arene complex. J Organomet Chem 2017;848:214–21. doi:10.1016/j.jorganchem.2017.08.003.

[27] Santi M, Mapanao AK, Cappello V, Voliani V. Production of 3D Tumor Models of Head and Neck Squamous Cell Carcinomas for Nanotheranostics Assessment. ACS Biomater Sci Eng 2020;6:4862–9. doi:10.1021/acsbiomaterials.0c00617.

[28] Mapanao AK, Voliani V. Three-dimensional tumor models: Promoting breakthroughs in nanotheranostics translational research. Appl Mater Today 2020;19:100552. doi:10.1016/j.apmt.2019.100552.

[29] Lu H, Blunden BM, Scarano W, Lu M, Stenzel MH. Anti-metastatic effects of RAPTA-C conjugated polymeric micelles on two-dimensional (2D) breast tumor cells and three-dimensional (3D) multicellular tumor spheroids. Acta Biomater 2016;32:68–76. doi:10.1016/j.actbio.2015.12.020.

[30] Savić A, Gligorijević N, Aranđelović S, Dojčinović B, Kaczmarek AM, Radulović S, et al. Antitumor activity of organoruthenium complexes with chelate aromatic ligands, derived from 1,10-phenantroline: Synthesis and biological activity. J Inorg Biochem 2020;202:110869. doi:10.1016/j.jinorgbio.2019.110869.

[31] Mitrović A, Kljun J, Sosič I, Gobec S, Turel I, Kos J. Clioquinol-ruthenium complex impairs tumour cell invasion by inhibiting cathepsin B activity. Dalt Trans 2016;45:16913–21. doi:10.1039/c6dt02369j.

[32] Pavlović M, Nikolić S, Gligorijević N, Dojčinović B, Aranđelović S, Grgurić-Šipka S, et al. New organoruthenium compounds with pyrido[2',3':5,6]pyrazino[2,3-f][1, 10]phenanthroline: synthesis, characterization, cytotoxicity, and investigation of mechanism of action. J Biol Inorg Chem 2019;24:297–310. doi:10.1007/s00775-019-01647-4.

[33] Cassano D, Santi M, D'Autilia F, Mapanao AK, Luin S, Voliani V. Photothermal effect by NIR-responsive excretable ultrasmall-in-nano architectures. Mater Horizons 2019;6:531–7. doi:10.1039/C9MH00096H.

[34] Cassano D, Mapanao A-K, Summa M, Vlamidis Y, Giannone G, Santi M, et al. Biosafety and Biokinetics of Noble Metals: The Impact of Their Chemical Nature. ACS Appl Bio Mater 2019;2:4464–70. doi:10.1021/acsabm.9b00630.

[35] Armanetti P, Pocoví-Martínez S, Flori A, Avigo C, Cassano D, Menichetti L, et al. Dual photoacoustic/ultrasound multi-parametric imaging from passion fruit-like nano-architectures. Nanomedicine Nanotechnology, Biol Med 2018;14:1787–95. doi:10.1016/j.nano.2018.05.007.

[36] Langhans SA. Three-Dimensional in Vitro Cell Culture Models in Drug Discovery and Drug Repositioning. Front Pharmacol 2018;9:1–14. doi:10.3389/fphar.2018.00006.

[37] Lin K, Zhao ZZ, Bo H Ben, Hao XJ, Wang JQ. Applications of ruthenium complex in tumor diagnosis and

therapy. Front Pharmacol 2018;9:1–10. doi:10.3389/fphar.2018.01323.